

MODELLING FLEXURAL BEHAVIOR OF PRECAST REINFORCED CONCRETE PILES

FEM PRC piles Members ○Thomas DROUIN¹ Susumu KONO¹ Taku OBARA¹
Flexural behavior Yoichi ASAI² Mitsumaru GOAN² David MUKAI³

1. Introduction

Damages to prestressed concrete piles during the 1995 Hyougoken-Nanbu earthquake¹⁾ has led to investigations over their ultimate behavior. This paper uses data from experiments on precast reinforced concrete (PRC) pile specimens²⁾. The purpose is to investigate flexural behavior of those piles through a finite element model, focusing on the moment and displacement capacity under various axial load ratios. The ultimate limit strain of concrete is also evaluated.

2. Finite element model

The two tested PRC piles were hollow, prestressed high-strength concrete piles : C_I_0 and C_I_2_①²⁾. They were identical, except for different axial load ratios of $\eta = 0$ and $\eta = 0.22$, respectively. Both specimens were modelled with line elements using fiber-type section discretization in OpenSees³⁾ software.

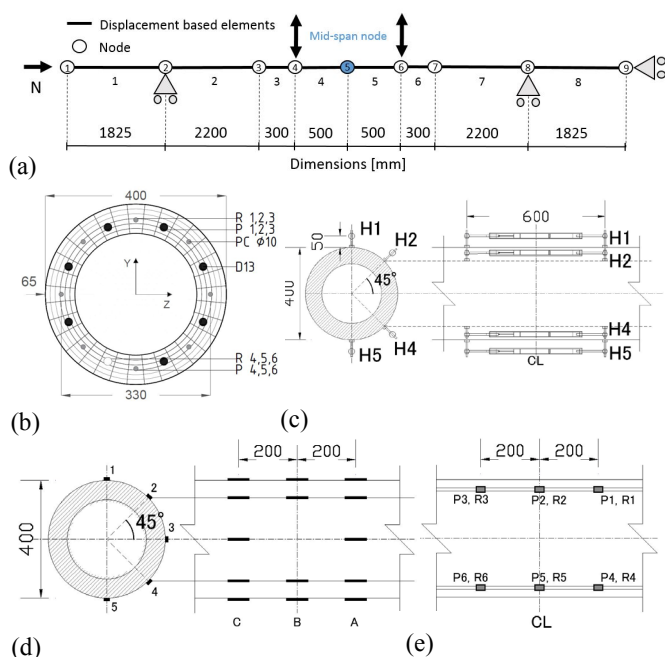


Fig. 1: PRC pile specimens in experiment and analysis: (a) FEM geometry, loading and boundary conditions, (b) fiber section of the elements, (c) location of displacement gauges to compute curvature (d) strain gauges on concrete and (e) strain gauges on prestressing tendons

Figure 1.a shows geometry, loading and boundary conditions of the model. The elements used are displacement-based beam-

column elements. Each displacement based element consist of 5 integration points, using the fiber section of Figure 1.b and Gauss-Lobatto integration method. The fiber section consist of 32 concrete fibers in the circumferential direction and 6 in the radial direction, resulting in 192 fibers. Prestressing tendons and mild reinforcement are modelled with 16 fibers. Second order P- Δ effects are considered in the solution using the geometric transformation.

3. Material models

Material properties in reference²⁾ are used. Both prestressed tendons and mild reinforcements are modelled using SteelMPF⁴⁾ model from OpenSees library (cf. figure 2.a), while the concrete is modelled with Concrete04⁵⁾, with degraded linear unloading/reloading stiffness according to the work of Karsan-Jirsa⁶⁾ and tensile strength with exponential decay $\alpha = 0.05$ (cf. figure 2.b). Parameters has been determined²⁾ from cylinder tests and splitting test for concrete, and tensile test for steel.

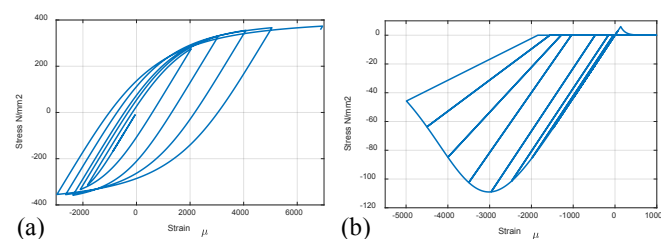


Fig. 2 Material models during cyclic loading in OpenSees: (a) SteelMPF and (b) Concrete04.

4. Analysis results

The vertical deflection of the mid-span (node 5) was controlled during the cyclic loading in experiment and analysis by incrementing the vertical displacement with loads applied at nodes 4 and 6. Moment, stress-strain and curvature in the mid-span section of the model are recorded at the right-end section of element 4. Moment in the mid-span during the experiment is calculated as the sum of the first order moment from applied lateral load, and the second order moment from recorded deformations and applied axial load. Curvature is obtained from the displacement gauge readings along the mid-span section (see figure 1.d).

Comparisons between experimental and analytical results are provided in figure 3.a and 4.a. A good agreement in the general behavior is observed. In terms of moment, the numerical model

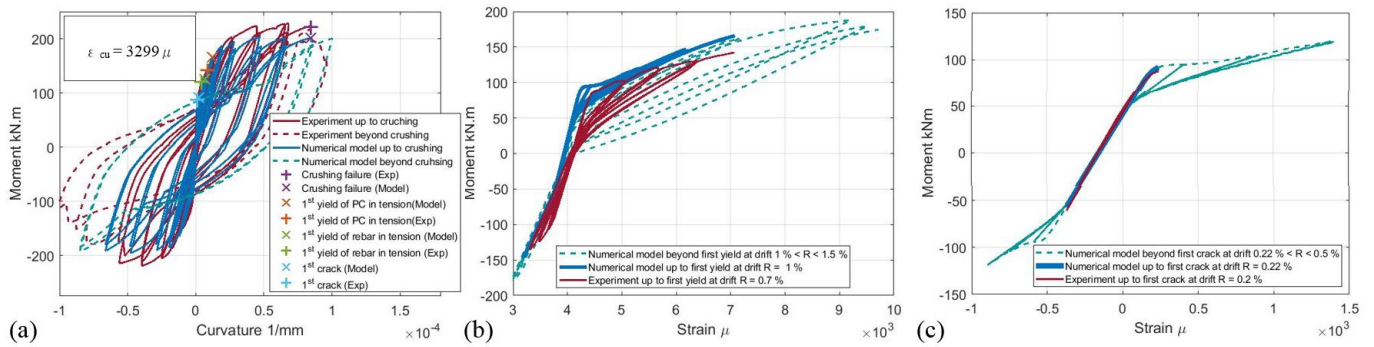


Fig 3 Specimen C_I_0 $\eta = 0$: comparison between numerical and experimental results : (a) moment-curvature, (b) moment-strain in prestressing tendons, (c) moment-strain in concrete.

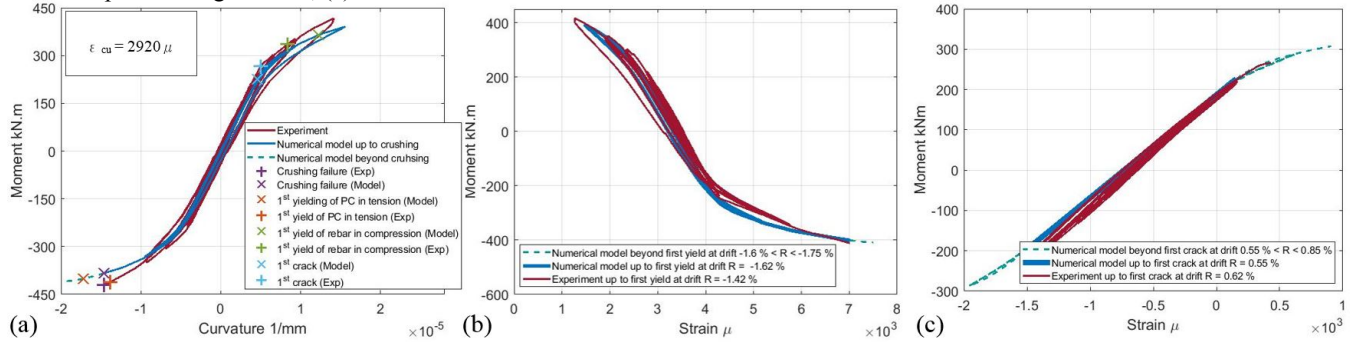


Fig 4 Specimen C_I_2 $\eta = 0.22$: comparison between numerical and experimental results : (a) moment-curvature, (b) moment-strain in prestressing tendons, (c) moment-strain in concrete.

slightly underestimates the moment capacity, with discrepancies in the range of -10 to -20 kN.m, which represent -10 % of the moment capacity at $\eta = 0$, and -6 % at $\eta = 0.22$.

The strain gauges readings of the prestressing tendons (cf. figure 1.e) up to the first yield are compared with the model in figure 3.b and 4.b. In these figures, the model is in agreement with the experiment, by assuming a perfect bond between prestressed tendons and concrete. The strain gauges readings of the surface concrete (cf. figure 1.d) up to the first crack are compared with the model in figure 3.c and 4.c. These figures show a good agreement between numerical model and experiment. Beyond the first plastic deformations, the accuracy of both concrete and steel model cannot be assessed from experiment because the strain gauges did not function.

5. Ultimate limit strain of concrete

The ultimate strain of concrete in the analysis is defined at the ultimate curvature observed in the experiment. According to the analysis, failure of C_I_0 ($\eta = 0$) occurred before reaching the peak strain $\epsilon_{p,1}$ of the concrete cylinder test, at a strain $\epsilon_{cu} = 2920 \mu$ ($0.97 \epsilon_{p,1}$) while failure of C_I_2 ($\eta = 0.22$) occurred after reaching the peak strain $\epsilon_{p,2}$ of the concrete cylinder test at a strain $\epsilon_{cu} = 3299 \mu$ ($1.04 \epsilon_{p,2}$). Discrepancies of these results needs to be investigated with additional specimens.

6. Conclusions

The model is able to accurately predict the pile's response in term of hysteresis degradation and material deformation, while its moment capacity predictions are slightly conservative.

Additional specimens will be modelled with higher axial load ratio, and tensile axial load. The results will be compared with the predictions using AIJ guideline's concrete models, in order to evaluate their safety and accuracy. Furthermore, the influence of other parameters such as pile diameter, thickness, and concrete strength will also be evaluated using this modelling approach.

Acknowledgments

This work was supported financially by JSPS through two Grant-in-Aid programs (PI: Shuji Tamura, and Susumu Kono). We are thankful to the Concrete Pile and Pole Industrial Technology Association for their expert advice and support. We are also thankful to the Collaborative Research Project (Materials and Structures Laboratory), and the World Research Hub Initiative (Institute of Innovative Research), at Tokyo Institute of Technology for their generous support.

References

- Horikoshi, K., Tateishi, A., and Ohtsu, H. (2000). "Detailed investigation of piles damaged by Hyogoken-Nambu earthquake." *Proc. 12th World Conference on Earthquake Engineering*, Auckland, New Zealand, Paper no. 2477.
- Asai Y. et al. (2017.7): Study on structural performance evaluation of concrete pile foundation structure system to ensure continuous usability after large earthquake, part 2, 3 & 4, Summaries of technical papers of annual meeting Architectural Institute of Japan, pp.577-582.
- OpenSees finite element software, v3.1.0 (2019) : <https://opensees.berkeley.edu/>
- Menegotto, M., and Pinto, P.E. (1973). Method of analysis of cyclically loaded RC plane frames including changes in geometry and non-elastic behavior of elements under normal force and bending. Preliminary Report IABSE, vol 13.
- Popovics, S. (1973). "A numerical approach to the complete stress strain curve for concrete." *Cement and concrete research*, 3(5), 583-599.
- Karsan, I. D., and Jirsa, J. O. (1969). "Behavior of concrete under compressive loading." *Journal of Structural Division ASCE*, 95(ST12).

1 Tokyo Institute of Technology
 2 Concrete Pile and Pole Industrial Technology Association
 3 University of Wyoming

1 東京工業大学
 2 一般社団法人 コンクリートパイル・ポール協会
 3 ワイオミング大学